

Nonmetallic Low-Temperature Normal State of $\text{K}_{0.70}\text{Fe}_{1.46}\text{Se}_{1.85}\text{Te}_{0.15}$

Kefeng Wang,^{1,*} Hyejin Ryu,^{1,2} Erik Kampert,³ M. Uhlarz,³ J. Warren,⁴ J. Wosnitza,^{3,5} and C. Petrovic^{1,2,†}

¹*Condensed Matter Physics and Materials Science Department,
Brookhaven National Laboratory, Upton, New York 11973, USA*

²*Department of Physics and Astronomy, Stony Brook University, Stony Brook, New York 11794-3800, USA*

³*Hochfeld-Magnetlabor Dresden (HLD), Helmholtz-Zentrum Dresden-Rossendorf, D-01314 Dresden, Germany*

⁴*Instrument Division, Brookhaven National Laboratory, Upton, New York 11973, USA*

⁵*Institut für Festkörperphysik, TU Dresden, D-01062 Dresden, Germany*

(Dated: March 2, 2022)

The normal-state in-plane resistivity below the zero-field superconducting transition temperature T_c and the upper critical field $\mu_0 H_{c2}(T)$ were measured by suppressing superconductivity in pulsed magnetic fields for $\text{K}_{0.70}\text{Fe}_{1.46}\text{Se}_{1.85}\text{Te}_{0.15}$. The normal-state resistivity ρ_{ab} is found to increase logarithmically with decreasing temperature as $\frac{T}{T_c} \rightarrow 0$. Similar to granular metals, our results suggest that a superconductor - insulator transition below zero-field T_c may be induced in high magnetic fields. This is related to the intrinsic real-space phase-separated states common to all inhomogeneous superconductors.

PACS numbers: 72.80.Ga, 72.20.Pa, 75.47.Np

INTRODUCTION

The normal-state properties (including pseudogap at the Fermi surface and proximity of magnetism at the phase diagrams) of unconventional superconductors such as high- T_c copper oxides, iron-pnictides/chalcogenides and heavy-fermions have received much attention [1]. The linear temperature dependence of the in-plane resistivity above T_c [2–4] is considered to be related to magnetic quantum criticality and antiferromagnetic fluctuations [5]. Since the normal (nonsuperconducting) states of interest appear under extremely high magnetic fields and at low temperatures ($T \rightarrow 0$), only a few studies were performed investigating the normal-state properties of high- T_c superconductors below T_c so far. In copper oxides examples include underdoped $\text{La}_{2-x}\text{Sr}_x\text{CuO}_4$ and $\text{Bi}_2\text{Sr}_{2-x}\text{La}_x\text{CuO}_6$, where $\rho(T)$ diverges logarithmically below T_c and where a superconductor - insulator transition (SIT) is induced in pulsed magnetic fields [6–9]. This came as a surprise since insulating state revealed by the magnetic-field induced breakdown of superconductivity was not expected in a conventional metal. Studies $(\text{Ba,K})\text{Fe}_2\text{As}_2$ and $\text{LaFeAsO}_{1-x}\text{F}_x$ resistivity suggested a slight upturn below zero-field T_c after the partial suppression of superconductivity up to 61 T pulsed field [10, 11]. In $\text{SmFeAsO}_{1-x}\text{F}_x$ magnetic-field induced logarithmic insulating behavior in the resistivity spans one decade in temperature above the zero-field T_c , stems from the large magnetoresistance that extends to temperatures well above the log-T regime and is not linked to the superconducting state [12].

$\text{K}_x\text{Fe}_{2-y}\text{Se}_2$ exhibits a high-temperature insulator-metal crossover at $T_s \sim 100 - 200$ K before becoming superconducting at $T_c = 30$ K [13–15]. Insulating ground states can also be found by tuning parameters such as Fe occupancy or isovalent S substitution on the

Se atomic site [16, 17]. As opposed to copper oxides, a dual description including both itinerant and localized carriers/magnetic moments may be required [18, 19]. But similar to the copper oxides, it is imperative to probe the normal state below zero-field T_c . This is even more so due to the argued granular-like superconductivity arising in nanoscale superconducting grains separated by non-superconducting islands, with a macroscopic superconducting condensate being established via Josephson tunneling among the grains [20, 21]. In the underdoped cuprates electronic granularity stems from the nature of the chemical bonds; hole-rich superconducting regions may form for low level of hole doping even though the crystal structure is not granular [22]. In $\text{K}_x\text{Fe}_{2-y}\text{Se}_2$ crystals, the phase separation is an intrinsic feature of the crystal structure [23, 24].

Here, we measured the normal-state in-plane resistivity below T_c for $\text{K}_{0.70}\text{Fe}_{1.46}\text{Se}_{1.85}\text{Te}_{0.15}$ by suppressing superconductivity in pulsed magnetic fields. The normal-state resistivity ρ_{ab} is found to increase logarithmically as $\frac{T}{T_c} \rightarrow 0$. Similar to granular superconductors and underdoped $\text{La}_{2-x}\text{Sr}_x\text{CuO}_4$ and $\text{Bi}_2\text{Sr}_{2-x}\text{La}_x\text{CuO}_6$ [6–9], our results suggest for the first time that magnetic-field-driven SIT is induced in high magnetic field in Fe-based superconductors.

EXPERIMENTAL

Single crystals of pure $\text{K}_x\text{Fe}_{2-y}\text{Se}_2$ and nominally 10% Te-doped $\text{K}_x\text{Fe}_{2-y}\text{Se}_2$ used in this study were grown and characterized as described previously [17]. The powder X-ray diffraction (XRD) spectra were taken with Cu K α radiation ($\lambda = 0.15418$ nm) by a Rigaku Miniflex X-ray machine, confirming phase purity. The cleaved surface image was determined in a JEOL JSM-6500 scanning

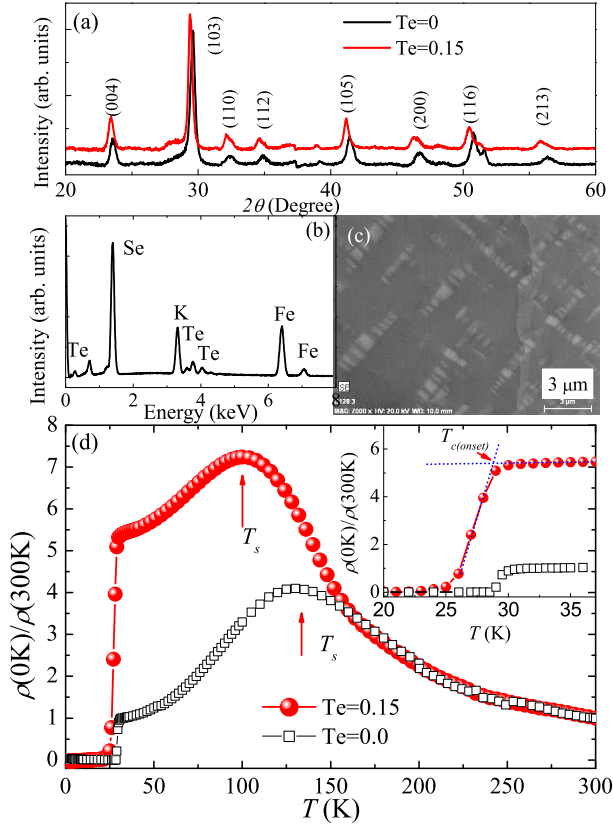


FIG. 1. (color online) Nominal 7.5% Te substitution of Se in $K_xFe_{2-y}Se_2$ induces a decrease of the superconducting transition temperature T_c and of the semiconductor-metal transition temperature T_s . (a) The powder x-ray diffraction patterns for Te-doped and pure $K_xFe_{2-y}Se_2$ crystals. The shift of the diffraction peaks toward lower angle shows the expanded lattice in Te-doped crystals. (b) The energy-dispersive X-ray spectroscopy of a typical $K_{0.70}Fe_{1.46}Se_{1.85}Te_{0.15}$ single crystal, which clearly shows the Te peak. (c) The SEM image of a typical single crystal showing stripe phases. (d) Temperature dependence of the resistivity for pure and Te-doped $K_xFe_{2-y}Se_2$. The inset shows the magnified part around the superconducting transition temperature. The $T_{c(onset)}$ decreases from 30 to 29.5 K and T_s decreases from 130 to 100 K.

electron microscope (SEM). The average stoichiometry was determined by energy-dispersive X-ray spectroscopy (EDX) in the same SEM. Four-probe resistivity was measured in pulsed magnetic fields up to 65 T and in Quantum Design PPMS-14 and PPMS-9. Contacts were attached to the ab plane of crystals in a glove box. Sample dimensions were measured by an optical microscope Nikon SMZ-800 with 10 μm resolution. The electric current used in the pulsed field measurement was always 2 mA and the corresponding electric current density in the sample was $\sim 1.39 \times 10^4$ A/m 2 .

RESULTS AND DISCUSSIONS

Fig. 1(a) shows the diffraction patterns of both compounds and all reflections can be indexed in the $I4/mmm$ space group. The lattice parameters for $K_{0.70}Fe_{1.46}Se_{1.85}Te_{0.15}$ from the refinement are $a = b = 3.910(3)$ nm and $c = 14.268(6)$ nm, which are larger than for $K_xFe_{2-y}Se_2$ ($a = b = 3.881(1)$ nm and $c = 14.151(6)$ nm). The expanded crystal lattice implies that Te enters the lattice, which is further confirmed by the EDX large-area elemental analysis which shows the average stoichiometry $K_{0.70(6)}Fe_{1.46(3)}Se_{1.84(8)}Te_{0.15(2)}$ [Fig. 1(b)]. The SEM image [Fig. 1(c)] shows a typical phase-separation pattern. Compared to undoped $K_xFe_{2-y}Se_2$ [25–27], the pattern is inhomogeneous: Stripes can be up to 100 nm large whereas their lower limit is below 50 nm. The local-point analysis on the background (dark) areas gives the stoichiometry $K_{0.78(4)}Fe_{1.70(3)}Se_{1.84(8)}Te_{0.15(2)}$, which is close to the 245 insulating phase [28]. About 7.5% Te substitution induces a $T_{c(onset)}$ decrease from ~ 30 K to ~ 29.5 K, and metal-semiconductor transition temperature, T_s , decrease from ~ 130 K to ~ 100 K [Fig. 1(d)].

Near T_c , the upper critical field slopes, $d\mu_0 H_{c2}(T)/dT|_{T=T_c}$ in $K_xFe_{2-y}Se_2$ and other ternary/quaternary iron arsenide and selenide superconductors, are about 5 to 12 TK^{-1} for $H\parallel ab$ and 1 to 3 TK^{-1} for $H\parallel c$. Using the Werthamer-Helfand-Hohenberg (WHH) estimate [29], results in $\mu_0 H_{c2}(T)|_{T=0} = (125\text{-}275)$ T and (30-60) T for $H\parallel ab$ and $H\parallel c$, respectively [30–32]. The upper critical field for $H\parallel c$ presents almost linear temperature dependence up to 60 T instead of the saturation predicted by WHH. This is ascribed to multiband effect [30, 31]. Although the upper critical field for $H\parallel c$ is larger than the WHH estimate, it is smaller than $\mu_0 H_{c2}(T)$ for $H\parallel ab$ which is well explained within the WHH theory [31, 32]. For $K_{0.70}Fe_{1.46}Se_{1.85}Te_{0.15}$, we observe similar slopes of $\mu_0 H_{c2}(T)$ with $d\mu_0 H_{c2}(T)/dT|_{T=T_c} \sim 2.1(4)$ TK^{-1} for $H\parallel c$ [Fig. 2(a-c)] and $d\mu_0 H_{c2}(T)/dT|_{T=T_c} \sim 4.9(3)$ TK^{-1} for $H\parallel ab$. However, in $K_{0.70}Fe_{1.46}Se_{1.85}Te_{0.15}$, at lower temperatures $\mu_0 H_{c2}(T)$ is significantly reduced. A magnetic field of 61 T suppresses the superconductivity at 1.7 K for $H\parallel c$, as opposed to $H\parallel a$ [Fig. 3(a)]. This is ascribed to a change in the temperature dependence of $\mu_0 H_{c2}(T)$.

Effects of Pauli spin paramagnetism and spin-orbit scattering can be included in the WHH theory for a single-band s-wave weak-coupling type-II superconductor in the dirty limit by adding the Maki parameters α and λ_{so} [29, 33]. Then, $\mu_0 H_{c2}(T)$ is given by

$$\ln\left(\frac{1}{t}\right) = \left(\frac{1}{2} + \frac{i\lambda_{so}}{4\gamma}\right)\psi\left(\frac{1}{2} + \frac{h + \lambda/2 + i\gamma}{2t}\right) + \left(\frac{1}{2} - \frac{i\lambda_{so}}{4\gamma}\right)\psi\left(\frac{1}{2} + \frac{h + \lambda/2 - i\gamma}{2t}\right) - \psi\left(\frac{1}{2}\right), \quad (1)$$

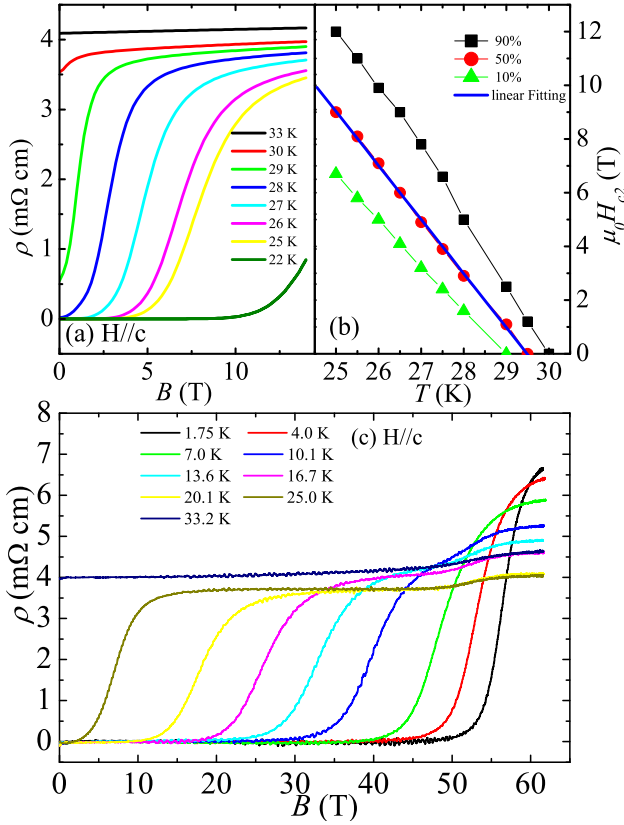


FIG. 2. (color online) Field dependence of the in-plane resistivity in a $\text{K}_{0.70}\text{Fe}_{1.46}\text{Se}_{1.85}\text{Te}_{0.15}$ single crystal with magnetic field applied parallel to the c axis at fixed temperatures. (a) The resistivity data for temperatures between 22 and ~ 33 K up to 14 T. (b) Temperature dependence of $\mu_0 H_{c2}(T)$ near zero-field T_c for the Te-doped crystal with $H||c$ using different criteria in the resistive transition shown in (a). (c) Resistivity data for temperatures between 1.75 and 33 K in pulsed fields up to 60 T.

where $\psi(x)$ is the digamma function, $\gamma = [(\alpha h)^2 - (\lambda_{so}/2)^2]^{1/2}$, and

$$h = \frac{4\mu_0 H_{c2}(T)}{\pi^2 T_c [-d\mu_0 H_{c2}(T)/dT]_{T=T_c}}. \quad (2)$$

In our data, we observe a convex curvature and a tendency to saturation for $\mu_0 H_{c2}(T)$ with $H||c$ at low temperatures [Fig. 3(b)] which can be well understood by the WHH theory with $\alpha = 0$ and $\lambda = 0$, i.e., with orbitally limited H_{c2} : $\mu_0 H_{c2}^*(0) = -0.693T_c(dH_{c2}/dT)_{T_c}$ [the blue curve in Fig. 3(b)]. Hence, the isovalent Te substitution suppresses the multiband character and promotes a single-band orbital-limited behavior.

The in-plane upper critical field is limited due to spin paramagnetism since $\alpha = 0.28$ and $\lambda_{so} = 0$ [red curve in Fig. 3(b)]. When compared to $\alpha_{H||ab} = 5.6$ and $\alpha_{H||ab} = 1.9$ in $\text{Tl}_{0.58}\text{Rb}_{0.42}\text{Fe}_{1.72}\text{Se}_2$ and $\text{K}_x\text{Fe}_{2-y}\text{Se}_2$, respectively [30, 32], the spin-paramagnetic effect in the Te-doped system is very

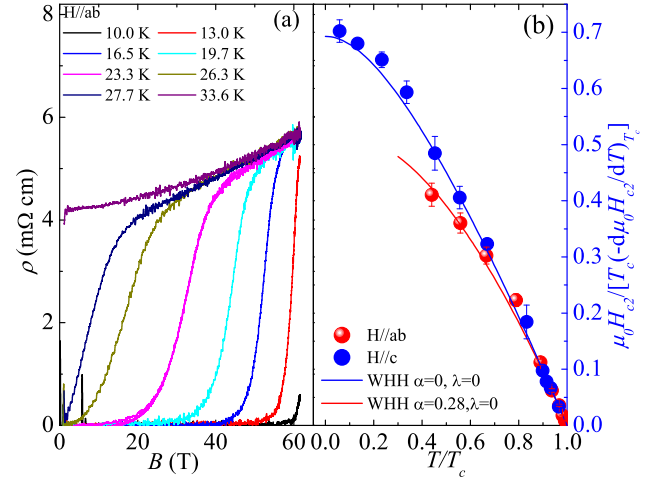


FIG. 3. (color online) The upper critical fields in $\text{K}_{0.70}\text{Fe}_{1.46}\text{Se}_{1.85}\text{Te}_{0.15}$ follow the temperature dependence as predicted by the WHH theory. (a) Field dependence of the in-plane resistivity of $\text{K}_{0.70}\text{Fe}_{1.46}\text{Se}_{1.85}\text{Te}_{0.15}$ for pulsed magnetic fields applied perpendicular to the c -axis. (b) Temperature dependence of the upper critical field $H_{c2}(T)$ (plotted as $\frac{\mu_0 H_{c2}}{T_c [-d\mu_0 H_{c2}/dT]_{T_c}}$) for magnetic fields parallel (circles) and perpendicular (balls) to the c axis, respectively. The solid lines are the fitting results using WHH theory with different parameters.

small ($\alpha < 1$), but the high anisotropy of $\mu_0 H_{c2}(T)$ for the different principal crystallographic directions remains, suggesting that an anisotropic Fermi surface is preserved. Open electron orbits along the c axis render an orbital-limited field unlikely and spin-paramagnetic effects should play an important role for $H||ab$. The paramagnetically limited field $\mu_0 H_{c2}^p(0)$ is given by $\mu_0 H_{c2}^p(0) = \mu_0 H_{c2}^*(0)/\sqrt{1 + \alpha^2}$ and $\alpha = \sqrt{2}H_{c2}^*(0)/H_p(0)$, where $\mu_0 H_p(0)$ is zero-temperature Pauli limited field and the orbitally limited $\mu_0 H_{c2}^*$ given above [33]. This gives $\mu_0 H_{c2}^{p,ab}(0) = 100$ T whereas $\mu_0 H_{c2}^{p,c}(0) = 45.7$ T. The zero-temperature coherence length, $\xi(0)$, can be estimated using the Ginzburg-Landau formula $\mu_0 H_{c2}(0) = \Phi_0/2\pi\xi^2(0)$, where $\Phi_0 = 2.07 \times 10^{-15}$ Wb, resulting $\xi(0)_{ab} = 2.7(1)$ nm and $\xi(0)_c = 1.8(3)$ nm, respectively.

The reduction of the Maki parameter, α , in $\text{K}_{0.70}\text{Fe}_{1.46}\text{Se}_{1.85}\text{Te}_{0.15}$ when compared to $\text{K}_x\text{Fe}_{2-y}\text{Se}_2$ cannot be explained by disorder effects since for electronic systems with more disorder one expects a larger α [34]. Therefore, another effect must compete and prevail over the disorder induced by Te substitution. With strong-coupling correction for electron-boson and electron-electron interactions $\mu_0 H_p(0) = 1.86(1 + \lambda)^\varepsilon \eta_\Delta \eta_{ib}(1 - I)$, where strong-coupling intraband corrections for the gap are described by η_Δ , I is the Stoner factor $I = N(E_F)J$, $N(E_F)$ is the electronic density of states (DOS) per spin at the Fermi level, E_F , J is an effective exchange integral, η_{ib} is introduced to describe phenomenologically the effect of the gap

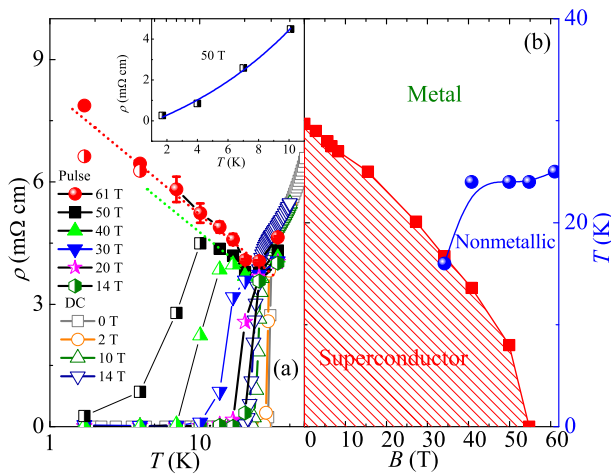


FIG. 4. (color online) (a) Temperature dependence of the in-plane resistivity in several DC (open symbols) and pulsed (filled symbols) magnetic fields for temperature between 1.75 and 100 K. Pulsed-field data (filled symbols) near T_c is consistent with results in DC and zero fields (open symbols). The two half-filled symbols for 61 T at 1.75 and 4 K denote the extrapolated values of the resistivity after complete suppression of the superconductivity. The red and green dashed lines are the linear fitting result for the 61 T data and 50 T data when using logarithmic scale, respectively. Inset: resistivity of the mixed state in 50 T field and the blue dotted line is an exponential fitting result (see text) (b) The schematic temperature-field phase diagram of $\text{K}_{0.70}\text{Fe}_{1.46}\text{Se}_{1.85}\text{Te}_{0.15}$.

anisotropy, λ is the electron-boson coupling constant and $\varepsilon = 0.5$ or 1 [35]. The spin-paramagnetic effect can be less pronounced when the Stoner factor becomes small which can be achieved through suppressing either the DOS at the Fermi level or the effective exchange integral J [35]. The reduction of both, the multiband character in $H_{c2}(T)$ and the spin paramagnetism when compared to pure $\text{K}_x\text{Fe}_{2-y}\text{Se}_2$, implies that electronic states, removed by Te substitution, carry substantial partial density of states at the Fermi level, i.e., that Te substitution reduces the occupancy of heavily renormalized d_{xy} orbitals [36].

In $\text{K}_{0.70}\text{Fe}_{1.46}\text{Se}_{1.85}\text{Te}_{0.15}$, a magnetic field of 61 T parallel to the c axis completely suppresses superconductivity above 1.75 K [Fig. 2(c) and 3(b)], providing the opportunity to study the normal-state properties as $T \rightarrow 0$. The application of 61 T leads to a negative $d\rho/dT$ resembling insulating rather than metallic behavior [Fig. 4(a)]. It is apparent that a SIT occurs right below T_c (filled balls) after the superconductivity is completely suppressed above H_{c2} . At 50 T, the resistivity as well shows SIT and is nearly identical to that at 61 T field until superconductivity sets in below about 15 K. We first note that the insulating behavior in high magnetic fields appears only below the zero-field T_c . It is also instructive to note that above the zero-field T_c the field dependence of the resistivity up to 61 T is minute for $H||c$, in contrast

to $\text{SmFeAsO}_{1-x}\text{F}_x$ [12]. The temperature-magnetic-field phase diagram for $\text{K}_{0.70}\text{Fe}_{1.46}\text{Se}_{1.85}\text{Te}_{0.15}$ is shown in Fig. 4(b).

A SIT was first reported in ultrathin, disordered and granular type-I superconductors [37, 38]. Then, a SIT with an insulating resistivity, increasing logarithmically below T_c , was reported in high- T_c cuprate superconductors utilizing pulsed magnetic fields [6–8]. Such a temperature dependence is different from variable range hopping (VRH) and thermally activated transport observed in semiconductors. Kondo-type magnetic scattering is also unlikely since the spin-flip scattering should be suppressed in 61 T. Evidence for an intrinsic electronic phase separation in the cuprate superconductors [39] suggests that the logarithmic increase in the resistivity and the SIT originates from an inhomogeneous state, presumably similar to granular Nb. [38, 40].

$\text{K}_x\text{Fe}_{2-y}\text{Se}_2$ features a highly defective crystal structure where the magnetic insulating regions are spatially intrinsically separated and coexist with superconducting regions on the a length scale of 100 nm to 1 μm [25–27]. However, as opposed to two-dimensional alternate stacking of insulating and (super)conducting layers, the stripe-type phase separation in $\text{K}_x\text{Fe}_{2-y}\text{Se}_2$ is more three-dimensional [21–23]. The conductivity in such inhomogeneous samples must include contributions from the insulating (σ_i) and metallic (σ_m) regions, i.e., $\sigma = \sigma_m + \sigma_i$. When $T < T_c$, σ_m goes to infinity due to superconductivity and the insulating part of the sample is short-circuited ($\sigma = \sigma_m = \infty$). But even around T_c and in particular in the normal state at high magnetic field when $T \rightarrow 0$, $\sigma \sim \sigma_m$ holds as well since insulating regions have a nearly two orders of magnitude higher resistivity [41]. This is consistent with the observation that insulating regions do not contribute to the spectral weight in angular resolved photoemission data close to E_F [36].

Therefore, superconductivity in $\text{K}_x\text{Fe}_{2-y}\text{Se}_2$ is similar to that in granular superconductors, namely a three-dimensional array of superconducting grains in an insulating matrix [38, 40]. Strong magnetic fields suppress superconductivity in each grain. The possible scenarios explaining a SIT include Anderson localization [42] and the bosonic scenario where the gap is driven to zero by phase fluctuations [43, 44]. The observed logarithmic divergence of the resistivity in the nonmetallic normal state of $\text{K}_{0.70}\text{Fe}_{1.46}\text{Se}_{1.85}\text{Te}_{0.15}$ [Fig. 4(a)] does not follow the VRH conduction which is observed for Anderson localization. In the bosonic scenario the Cooper pairs are localized in granules (similar to defects). For a $H > H_{c2}$, virtual Cooper pairs may form, leading to a reduction of the DOS. When $T \rightarrow 0$, the pairs cannot travel between grains and the resistivity becomes much larger than for a normal metal without electron-electron interactions [43, 44]. In contrast to the spin-paramagnetic critical field, the orbital critical field de-

depends on the grain size as $H_{c2}^o \sim \phi_0/R\xi$ where R is the average grain radius and ξ is the coherence length. Since the upper critical field in $\text{K}_{0.70}\text{Fe}_{1.46}\text{Se}_{1.85}\text{Te}_{0.15}$ is about 55(3) T and the grain coherence length is 2.7(1) nm, we estimate a lower limit of the stripe grain size to be $R = 21(2)$ nm. Near the SIT on superconducting side it is expected that $\rho = \rho_0 \exp(T/T_0)$ [40] in high fields due to the destruction of fluctuating quasilocalized Cooper pairs and a concomitant increase of the number of quasiparticles at the Fermi level. Our 50 T resistivity data in the mixed state can be described well by this formula [The blue line in inset of Fig. 4(a)]. Different heat treatment and quenching can bring about changes in the normal-state resistivities, arrangement and connectivity of the superconducting grains [28]. This can influence the tunneling conductance in the granular array and, therefore, it would be of great interest to study superconducting fluctuations in such samples in high magnetic fields in the normal state below T_c for further comparison with theory [38, 40].

Even though the logarithmic temperature dependence of the resistivity in copper oxides is consistent with the theory of granular superconductivity if electrons in different CuO planes are incoherent in the low-temperature limit [45, 46], this is still controversial since the SIT in copper oxides occurs on the metallic side of the Mott limit ($k_F l > 1$, where k_F is the Fermi wave vector and l is the mean free path) [47]. Approaches offered to explain insulating states in copper-oxide superconductors postulate spin-charge separation [48], invoke a bipolaron theory of strongly correlated Mott-Hubbard insulators [49], or propose Mott insulating states in antiferromagnetic vortices within the framework of SO(5) theory of antiferromagnetism and superconductivity [50]. In the light of increasing evidence for insulating states in the different kinds of high- T_c superconductors in pulsed magnetic fields, more theoretical work may be needed to determine which of these approaches is compatible with real-space and/or electronic phase separation in materials of different structure and bonding types.

CONCLUSION

In summary, the normal-state in-plane resistivity and the upper critical fields of $\text{K}_{0.70}\text{Fe}_{1.46}\text{Se}_{1.85}\text{Te}_{0.15}$ are measured by suppressing superconductivity in pulsed magnetic fields. The temperature dependence of $\mu_0 H_{c2}(T)$ can be well described using the WHH theory, in contrast to $\text{K}_x\text{Fe}_{2-y}\text{Se}_2$ where the linear temperature dependence signals multiband effects. After suppressing superconductivity, the normal-state resistivity, ρ_{ab} , is found to be insulating and to diverge logarithmically as $\frac{T}{T_c} \rightarrow 0$. Similar to the SIT in granular superconductors, our results suggest that the mechanism for the SIT in high magnetic fields is related to intrinsic phase-separated states

in this kind of materials.

ACKNOWLEDGMENTS

We thank Myron Strongin and Dragana Popovic for useful discussions. Work at Brookhaven is supported by the U.S. DOE under contract No. DE-AC02-98CH10886. We acknowledge the support of the HLD at HZDR, member of the European Magnet Field Laboratory. CP acknowledges support by the Alexander von Humboldt Foundation.

* kwang@bnl.gov

† petrovic@bnl.gov

- [1] D. J. Scalapino, *A common thread: The pairing interaction for unconventional superconductors.*, Rev. Mod. Phys. **84**, 1383 (2012).
- [2] H. Takagi, *Systematic evolution of temperature-dependent resistivity in $\text{La}_{2-x}\text{Sr}_x\text{CuO}_4$* , Phys. Rev. Lett. **69**, 2975 (1992).
- [3] R. Daou, David LeBoeuf, N. Doiron-Leyraud, S.Y. Li, F. Laliberté, O. Cyr-Choinière, Y.J. Jo, L. Balicas, J.-Q. Yan, J.-S. Zhou, J.B. Goodenough, and L. Taillefer, *Linear temperature dependence of resistivity and change in the Fermi surface at the pseudogap critical point of a high- T_c superconductor*, Nat. Phys. **5**, 31 (2009).
- [4] P. Gegenwart, Qimiao Si and F. Steglich, *Quantum criticality in heavy-fermion metals*, Nat. Physics **4**, 186 (2008).
- [5] H. v. Löhneysen, A. Rosch, M. Vojta and P. Wölfle, *Fermi-liquid instabilities at magnetic quantum phase transitions*, Rev. Mod. Phys. **79**, 1015 (2009).
- [6] Y. Ando, G. S. Boebinger, A. Passner, T. Kimura, and K. Kishio, *Logarithmic Divergence of both In-Plane and Out-of-Plane Normal-State Resistivities of Superconducting $\text{La}_{2-x}\text{Sr}_x\text{CuO}_4$ in the Zero-Temperature Limit.*, Phys. Rev. Lett. **75**, 4662 (1995).
- [7] G. S. Boebinger, Y. Ando, A. Passner, T. Kimura, M. Okuya, J. Shimoyama, K. Kishio, K. Tamasaku, N. Ichikawa, and S. Uchida, *Insulator-to-Metal Crossover in the Normal State of $\text{La}_{2?x}\text{Sr}_x\text{CuO}_4$ Near Optimum Doping*, Phys. Rev. Lett. **77**, 5417 (1996).
- [8] S. Ono, Y. Ando, T. Murayama, F. F. Balakirev, J. B. Betts, and G. S. Boebinger, *Metal-to-Insulator Crossover in the Low-Temperature Normal State of $\text{Bi}_2\text{Sr}_{2-x}\text{La}_x\text{CuO}_{6+\delta}$* , Phys. Rev. Lett. **85**, 638 (2000).
- [9] Xiaoyan Shi, G. Logvenov, A. T. Bollinger, I. Božović, C. Panagopoulos, and Dragana Popović, *Emergence of superconductivity from the dynamically heterogeneous insulating state in $\text{La}_{2-x}\text{Sr}_x\text{CuO}_4$* , Nature Mater. **12**, 47 (2013).
- [10] H. Q. Yuan, J. Singleton, F. F. Balakirev, S. A. Baily, G. F. Chen, J. L. Luo, and N. L. Wang, *Nearly isotropic superconductivity in $(\text{Ba},\text{K})\text{Fe}_2\text{As}_2$* , Nature **457**, 565 (2009).
- [11] Y. Kohama, Y. Kamihara, A. Baily, L. Civale, S. C. Riggs, F. F. Balakirev, T. Atake, M. Jaime, M. Hirano

- and H. Hosono, Nearly isotropic superconductivity in (Ba,K)Fe₂As₂, *Nature* **457**, 565 (2009).
- [12] S. C. Riggs, J. B. Kemper, Y. Jo, Z. Stegen, L. Balicas, G. S. Boebinger, F. F. Balakirev, A. Migliori, H. Chen, R. H. Liu and X. H. Chen, Magnetic field-induced log-T insulating behavior in the resistivity of fluorine-doped SmFeAsO_{1-x}F_x, *Phys. Rev. B* **79**, 212510 (2009).
- [13] J. Guo, S. Jin, G. Wang, S. Wang, K. Zhu, T. Zhou, M. He, and X. L. Chen, *Superconductivity in the iron selenide K_xFe₂Se₂ (0 ≤ x ≤ 1.0)*, *Phys. Rev. B* **82**, 180520 (2010).
- [14] E. Dagotto, *The unexpected properties of alkali metal iron selenide superconductors*, *Rev. Mod. Phys.* **85**, 849 (2013).
- [15] H.-H. Wen, *Overview on the physics and materials of the new superconductor K_xFe_{2-y}Se₂*, *Rep. Prog. Phys.* **75**, 112501 (2012).
- [16] Y. J. Yan, M. Zhang, A. F. Wang, J. Ying, Z. Y. Li, W. Qin, X. G. Guo, J. Q. Li, Jianping Hu and X. H. Chen, *Electronic and magnetic phase diagram in K_xFe_{2-y}Se₂ superconductors*, *Sci. Rep. 2*, 212 (2012).
- [17] H. C. Lei, M. Abeykoon, E. S. Bozin, K. F. Wang, J. B. Warren, and C. Petrovic, *Phase Diagram of K_xFe_{2-y}Se_{2-z}S_z and the Suppression of its Superconducting State by an Fe₂-Se/S Tetrahedron Distortion*, *Phys. Rev. Lett.* **107**, 137002 (2011).
- [18] P. C. Dai, J. P. Hu, and E. Dagotto, *Magnetism and its microscopic origin in iron-based high-temperature superconductors*, *Nat. Phys.* **8**, 709 (2012).
- [19] Rong Yu and Qimiao Si, *Orbital-Selective Mott Phase in Multiorbital Models for Alkaline Iron Selenides K_{1-x}Fe_{2-y}Se₂*, *Phys. Rev. Lett.* **110**, 146402 (2013).
- [20] M. Sigrist and T. M. Rice, *Paramagnetic Effect in High T_c Superconductors - A Hint for d-wave Superconductivity*, *J. Phys. Soc. Jpn.* **61**, 4283 (1992).
- [21] R. H. Yuan, et al., *Nanoscale phase separation of antiferromagnetic order and superconductivity in K_{0.75}Se_{1.75}Se₂*, *Sci. Rep.* **2**, 221 (2012).
- [22] V. J. Emery and S.A. Kivelson, *Frustrated electronic phase separation and high-temperature superconductors*, *Physica C* **209**, 597 (1993).
- [23] Despina Louca, K. Park, B. Li, J. Neufeind and Jiaqiang Yan, *The hybrid lattice of K_xFe_{2-y}Se₂ : where superconductivity and magnetism coexist*. *Sci. Rep.* **3**, 2047 (2013).
- [24] F. Chen, M. Xu, Q. Q. Ge, Y. Zhang, Z. R. Ye, L. X. Yang, J. Jiang, B. P. Xie, R. C. Che, M. Zhang, A. F. Wang, X. H. Chen, D. W. Shen, J. P. Hu, and D. L. Feng, *Electronic Identification of the Parental Phases and Mesoscopic Phase Separation of K_xFe_{2-y}Se₂ Superconductors*, *Phys. Rev. X* **1**, 021020 (2011).
- [25] D. H. Ryan, W. N. Rowan-Weetaluktuk, J. M. Cadowan, R. Hu, W. E. Straszheim, S. L. Budko, and P. C. Canfield, *⁵⁷Fe Mössbauer study of magnetic ordering in superconducting K_{0.80}Fe_{1.76}Se_{2.00} single crystals*, *Phys. Rev. B* **83**, 104526 (2011).
- [26] Z. Wang, Y. J. Song, H. L. Shi, Z. W. Wang, Z. Chen, H. F. Tian, G. F. Chen, J. G. Guo, H. X. Yang, and J. Q. Li, *Microstructure and ordering of iron vacancies in the superconductor system K_yFe_xSe₂ as seen via transmission electron microscopy*, *Phys. Rev. B* **83**, 140505 (2011).
- [27] Wei Li, H. Ding, P. Deng, K. Chang, C. Song, Ke He, L. Wang, X. Ma, J. P. Hu, X. Chen and Q.K. Xue, *Phase separation and magnetic order in K-doped iron selenide superconductor*, *Nature* **8**, 126 (2012).
- [28] Xiaxin Ding, Delong Fang, Zhenyu Wang, Huan Yang, Jianzhong Liu, Qiang Deng, Guobin Ma, Chong Meng, Yuhui Hu and Hai-Hu Wen, *Influence of microstructure on superconductivity in K_xFe_{2-y}Se₂ and evidence for a new parent phase K₂Fe₇Se₈*, *Nat. Communications* **4**, 1897 (2013).
- [29] N. R. Werthamer, E. Helfand and P. C. Hohenberg, *Temperature and purity dependence of the superconducting critical field, H_{c2}.III. Electron spin and spin-orbit effects*, *Phys. Rev. B* **147**, 295 (1966).
- [30] L. Jiao, Y. Kohama, J. L. Zhang, H. D. Wang, B. Maiorov, F. F. Balakirev, Y. Chen, L. N. Wang, T. Shang, M. H. Fang, and H. Q. Yuan, *Phys. Rev. B* **85**, 064513 (2012).
- [31] E. D. Mun, M. M. Altarawneh, C. H. Mielke, V. S. Zapf, Rongwei Hu, S. L. Bud'ko and P.C. Canfield, *Anisotropic H_{c2} of K_{0.8}Fe_{1.76}Se₂ determined up to 60 T*, *Phys. Rev. B* **83**, 100514 (2011).
- [32] V. A. Gasparov, A. Audouard, L. Drigo, A. I. Rodigin, C. T. Lin, W. P. Liu, M. Zhang, A. F. Wang, X. H. Chen, H. S. Jeevan, J. Maiwald and P. Gegenwart, *Upper critical magnetic field in K_{0.83}Fe_{1.83}Se₂ and Eu_{0.5}K_{0.5}Fe₂As₂ single crystals*, *Phys. Rev. B* **87**, 094508 (2013).
- [33] K. Maki, *Effect of Pauli Paramagnetism on Magnetic Properties of High-Field Superconductors*, *Phys. Rev.* **148**, 362 (1966).
- [34] G. Fuchs, S.-L. Drechsler, N. Kozlova, G. Behr, A. Köhler, J. Werner, K. Nenkov, C. Hess, R. Klingeler, J. E. Hamann-Borrero, A. Kondrat, M. Grobosch, A. Narduzzo, M. Knupfer, J. Freudenberger, B. Büchner, and L. Schultz, *High-Field Pauli-Limiting Behavior and Strongly Enhanced Upper Critical Magnetic Fields near the Transition Temperature of an Arsenic-Deficient LaO_{0.9}F_{0.1}FeAs_{1-δ} Superconductor.*, *Phys. Rev. Lett.* **101**, 237003 (2008).
- [35] T. P. Orlando, E. J. McNiff, S. Foner, and M. R. Beasley, *Critical fields, Pauli paramagnetic limiting, and material parameters of Nb₃Sn and V₃Si*, *Phys. Rev. B* **19**, 4545 (1979).
- [36] M. Yi, D. H. Lu, R. Yu, S. C. Riggs, J. H. Chu, B. Lv, Z. K. Liu, M. Lu, Y. T. Cui, M. Hashimoto, S.-K. Mo, Z. Hussain, C. W. Chu, I. R. Fisher, Q. Si and Z.-X. Shen, *Observation of Temperature-Induced Crossover to an Orbital-Selective Mott Phase in A_xFe_{2-y}Se₂ (A = K, Rb) Superconductors*, *Phys. Rev. Lett.* **110**, 067003 (2013).
- [37] M. Strongin, R. S. Thompson, O. F. Kammerer, and J. E. Crow, *Destruction of Superconductivity in Disordered Near-Monolayer Films*, *Phys. Rev. B* **1**, 1078 (1970).
- [38] I. S. Beloborodov, A. V. Lopatin, V. M. Vinokur and K. B. Efetov, *Granular electronic systems*, *Rev. Mod. Phys.* **79**, 469 (2007).
- [39] K. M. Lang, V. Madhavan, J. E. Hoffman, H. Eisaki, S. Uchida, and J. C. Davis, *Imaging the granular structure of high-T_c superconductivity in underdoped Bi₂Sr₂CaCu₂O_{8+δ}*, *Nature* **415**, 412 (2002).
- [40] V. F. Gantmakher and V. T. Dolgoplov, *Superconductor-insulator quantum phase transition*, *Physics-Uspekhi* **53**, 1 (2010).
- [41] D. P. Shoemaker, D. Y. Chung, H. Claus, M. C. Francisco, S. Avci, A. Llobet, and M. G. Kanatzidis, *Phase relations in K_xFe_{2-y}Se₂ and the structure of superconducting K_xFe₂Se₂ via high-resolution synchrotron diffraction*,

- Phys. Rev. B **86**, 184511 (2012).
- [42] A. M. Finkelstein, *Suppression of superconductivity in homogeneously disordered systems*, Physica B **197**, 636 (1994).
- [43] I. S. Beloborodov, K. B. Efetov, and A. I. Larkin, *Magneto-resistance of granular superconducting metals in a strong magnetic field*, Phys. Rev. B **61**, 9145 (2000).
- [44] I. S. Beloborodov and K. B. Efetov, *Negative Magnetoresistance of Granular Metals in a Strong Magnetic Field*, Phys. Rev. Lett. **82**, 3332 (1999).
- [45] I. S. Beloborodov, K. B. Efetov, A. V. Lopatin, and V. M. Vinokur, *Transport Properties of Granular Metals at Low Temperatures*, Phys. Rev. Lett. **91**, 246801 (2003).
- [46] Z.-H. Pan, P. Richard, Y. M. Xu, M. Neupane, P. Bishay, A. V. Fedorov, H. Luo, L. Fang, H. H. Wen, Z. Wang, and H. Ding, *Evolution of Fermi surface and normal-state gap in the chemically substituted cuprates $\text{Bi}_2\text{Sr}_{2-x}\text{Bi}_x\text{CuO}_{6+\delta}$* , Phys. Rev. B **79**, 092507 (2009).
- [47] Y. Ando, *Implication of the Mott-limit violation in high- T_c cuprates*, J. Phys. Chem. Solids **69**, 3195 (2008).
- [48] V. J. Emery, S. A. Kivelson, and O. Zachar, *Spin-gap proximity mechanism of high-temperature superconductivity*, Phys. Rev. B **56**, 6120 (1997).
- [49] A. S. Alexandrov, V. V. Kabanov, and N. F. Mott, *Coherent ab and c transport theory of high- T_c cuprates*, Phys. Rev. Lett. **77**, 4796 (1996).
- [50] E. Demler, W. Hanke, and S.-C. Zhang, *$SO(5)$ theory of antiferromagnetism and superconductivity*, Rev. Mod. Phys. **76**, 909 (2004).